Trace gas fluxes from tidal salt marsh soils: implications for carbon-sulfur biogeochemistry

Margaret Capooci[1] and Rodrigo Vargas [1]

[1] Department of Plant and Soil Science
University of Delaware
152 Townsend Hall
531 South College Ave.
Newark, DE, USA 19716

Correspondence to:
Rodrigo Vargas
152 Townsend Hall
531 South College Ave.,
Newark, DE 19716
rvargas@udel.edu
Phone: 302-831-1386

Abstract

Tidal salt marsh soils can be a dynamic source of greenhouse gases such as carbon dioxide (CO_2), methane (CH_4), and nitrous oxide (N_2O), as well as sulfur-based trace gases such as carbon disulfide (CS_2) and dimethylsulfide (DMS) which play roles in global climate and carbon-sulfur biogeochemistry. Due to the difficulty in measuring trace gases in coastal ecosystems (e.g., flooding, salinity), our current understanding is based on snap-shot instantaneous measurements (e.g., performed during daytime low tide) which complicates our ability to assess the role of these ecosystems for natural climate solutions. We performed continuous, automated measurements of soil trace gas fluxes throughout the growing season to obtain high-temporal frequency data and to provide insights into magnitudes and temporal variability across rapidly changing conditions such as tidal cycles. We found that soil CO_2 fluxes did not show a consistent diel pattern, CH_4, N_2O, and CS_2 fluxes were highly variable with frequent pulse emissions (>2,500%, >10,000%, and >4,500% change, respectively), and DMS fluxes only occurred mid-day with changes >185,000%. When we compared continuous measurements with discrete temporal measurements (during daytime, at low tide), discrete measurements of soil CO_2 fluxes were comparable with those from continuous measurements, but misrepresent the temporal variability and magnitudes of CH_4, N_2O, DMS, and CS_2. Discrepancies between the continuous and discrete measurement data result in differences for calculating the sustained global warming potential (SGWP), mainly by an overestimation of CH_4 fluxes when using discrete measurements. The high temporal variability of trace gas fluxes complicates the accurate calculation of budgets for use in blue carbon accounting and earth system models.

1. Introduction

Coastal vegetated ecosystems such as tidal salt marshes, mangrove forests, and seagrass beds provide a wide range of ecosystem services, such as mitigating storm surge and providing nursery areas for fish species (Barbier et al., 2011; Möller et al., 2014). They also can potentially store large amounts of carbon at rates forty times higher than tropical rainforests ~~(Rosentreter et al., 2018; Duarte et al., 2005)~~(Rosentreter et al., 2018; Duarte et al., 2005) and are referred to as "blue carbon" ecosystems. The importance of coastal vegetated ecosystems in climate change policies has been recognized by the Paris Agreement (UNFCCC, 2015). Prior to the Paris Agreement, there has been increased interest in better quantifying the net balance between carbon storage and carbon release in coastal vegetated ecosystems for both scientific and carbon market purposes. For example, the Verified Carbon Standard developed a methodology to assess and verify the amount of carbon removed from the atmosphere in tidal wetland and seagrass restoration projects for carbon market purposes (Emmer et al., 2021). However, there are major knowledge gaps in assessing blue carbon in coastal vegetated ecosystems. Specifically, the high spatial and temporal variability of greenhouse gas (GHG) emissions, particularly for CH_4 and N_2O, in coastal vegetated ecosystems complicates blue carbon offset calculations ~~(Rosentreter et al., 2021; Capooci et al., 2019; Al-Haj and Fulweiler, 2020; Murray et al., 2015)~~(Rosentreter et al., 2021; Capooci et al., 2019; Al-Haj and Fulweiler, 2020; Murray et al., 2015). Thus, there is a need for developing measurement protocols to fully quantify the contribution of multiple GHGs in blue carbon ecosystems.

To improve our understanding of blue carbon ecosystems in global biogeochemical cycles we need to think beyond traditional GHG trace gases (i.e., CO_2, CH_4, N_2O). Tidal salt marshes produce sulfur-based trace gases due to the prevalence of sulfur cycling within their

soils, which has implications for carbon-sulfur biogeochemistry and the global climate. While

coastal areas are major sources of sulfur gases (Kellogg et al., 1972), there is large

uncertainty in emission rates ~~(Carroll et al., 1986; Andreae and Jaeschke, 1992).~~(Carroll et al.,

1986; Andreae and Jaeschke, 1992; Brimblecombe, 2014). Dimethyl sulfide (DMS) is one of the

dominant sulfur-based gases emitted from salt marshes (Hines, 1996)~~, and~~

~~dimethylsulfoniopropionate (DMSP), a DMS precursor, can be produced by salt marsh plant~~

~~species *Spartina alterniflora*, *S.*~~ and is considered a climate cooling gas, in part due to its

oxidation to SO_4 in the atmosphere (Thomas et al., 2010; Watts, 2000; Charlson et al., 1987).

Dimethylsulfoniopropionate (DMSP), a DMS precursor, can be produced by salt marsh plant

species *Spartina alterniflora, S. anglica*, and *S. foliosa* (Hines, 1996). DMS plays an important

role in linking together carbon and sulfur biogeochemistry in salt marsh soils. It can be

decomposed by not only sulfate-reducing bacteria, but can also act as a non-competitive

substrate for methylotrophic methanogenesis ~~(Kiene, 1988; Kiene and Visscher, 1987; Oremland~~

~~et al., 1982)~~(Kiene, 1988; Kiene and Visscher, 1987; Oremland et al., 1982) which allows

methane production to occur in soils dominated by sulfate reduction (Seyfferth et al., 2020).

~~Another sulfur-based trace gas released from tidal salt marshes is carbon disulfide (CS_2). CS_2 can~~

~~be produced by biological processes (Brimblecombe, 2014) and~~Another sulfur-based trace gas

released from tidal salt marshes is carbon disulfide (CS_2), which has an insignificant global

warming potential and a short atmospheric lifetime (Brühl et al., 2012). However, CS_2 is a

precursor to carbonyl sulfide (COS; Whelan et al., 2013). COS is the most abundant reduced

sulfur compound in the atmosphere and can form sulfate aerosols that affect the Earth's radiative

properties by reflecting sunlight, thereby having a cooling effect on the climate ~~(Watts, 2000;~~

~~Taubman and Kasting, 1995).~~(Watts, 2000; Taubman and Kasting, 1995). Despite sulfur-based

88   trace gases playing a role in wetland soil biogeochemistry and in global climate, there is a need

89   to quantify coastal wetland sulfur emissions and to connect those emissions to both the salt

90   marsh sulfur cycle and to global budgets (DeLaune et al., 2002; Whelan et al., 2013).

91   Historically, both soil GHGs and S-based fluxes are measured using manual survey

92   chambers, particularly during daytime low tide (e.g., De Mello et al., 1987) when soils are less

93   likely to be submerged and are accessible to researchers. Measurements at high tide in salt

94   marshes are difficult due to both reduced access to the marsh platform and reduced fluxes. Gases

95   from the soil mix with the overlying water column and move more slowly through water

96   compared to air, contributing to a decline in fluxes during high tide (Moffett et al., 2010).

97   Manual measurements have a number of advantages, including the ability to sample over large

98   areas over short periods of time (Moseman-Valtierra et al., 2016; Simpson et al., 2019), but these

99   measurements are labor-intensive and provide limited information regarding temporal variability

100   (Koskinen et al., 2014; Savage et al., 2014; Vargas et al., 2011). On the other hand, recent

101   advances in high temporal-frequency soil efflux measurements ~~(Capooci and Vargas, 2022;~~

102   ~~Diefenderfer et al., 2018; Järveoja et al., 2018)~~(Capooci and Vargas, 2022; Diefenderfer et al.,

103   2018; Järveoja et al., 2018) have provided researchers with unprecedented temporal information

104   to better understand diel and tidal patterns, as well as the influence of pulse events on trace gas

105   emissions within salt marshes. While the use of automated systems is becoming more common

106   in measuring salt marsh fluxes~~,~~ (Capooci and Vargas, 2022; Diefenderfer et al., 2018; Trifunovic

107   et al., 2020), their use is limited by high instrumentation costs, electricity requirements, and

108   logistical challenges associated with installing these instruments in an environment prone to

109   flooding and with high humidity. As automated systems become more prevalent, it provides

110   researchers with the opportunity to evaluate data collected from manual measurements, such as

111 daily means, that have been used to inform models and budgets, particularly for understudied

112 trace gases such as N_2O, CS_2, and DMS.

113   The objective of this study is to characterize the spatial and temporal variability of trace

114 gases from soils in a tidal salt marsh. Specifically, we focus on CO_2, CH_4, N_2O, CS_2, and DMS

115 to assess the differences between measurements taken at a particular time of day (i.e., daytime

116 low tide) and measurements with high-temporal frequency (i.e., continuous hourly measurements

117 for ~72 hours). Few studies have measured GHG fluxes from tidal salt marshes using

118 continuous, automated measurements (Diefenderfer et al., 2018; Capooci and Vargas,

119 2022)(Diefenderfer et al., 2018; Capooci and Vargas, 2022), and this is a pioneering study that

120 provides unprecedented information about the magnitudes and patterns of CS_2 and DMS fluxes

121 via continuous measurements. Furthermore, this study tests whether traditional measurement

122 protocols based on discrete temporal measurements provide similar information as data derived

123 from continuous measurements, including the calculation of the sustained global warming

124 potential (SGWP). Development of new technologies and incorporation of this information has

125 important implications for calculating greenhouse and trace gas budgets, as well as the role salt

126 marshes play in global biogeochemical cycles.

127

128 **2. Materials and methods**

129

130 *2.1 Study site*

131   The study was conducted at St. Jones Reserve, the brackish estuarine component of the

132 Delaware National Estuarine Research Reserve. The site is part of the Delaware Estuary and is

133 tidally connected to the Delaware Bay via the St. Jones River. St. Jones is classified as a

134   mesohaline tidal salt marsh (DNREC, 1999) and has silty clay loam soils (10% sand, 61% silt,

135   29% loam, Capooci et al 2019). The study was conducted in a section of the marsh dominated by

136   *Spartina alterniflora* (= *Sporobolus alterniflorus* (Loisel.); Peterson et al., 2014) and will be

137   referred to as SS as established in previous studies ~~(Seyfferth et al., 2020; Capooci and Vargas,~~

138   ~~2022)~~(Seyfferth et al., 2020; Capooci and Vargas, 2022). This area is lower in elevation relative

139   to the rest of the marsh, is characterized by sulfur reduction (Seyfferth et al., 2020), and covers

140   ~66% of the salt marsh landscape ~~(Vázquez-Lule and Vargas, 2021)~~(Vázquez-Lule and Vargas,

141   2021). The SS site rarely floods during high tide due to its distance from the tidal creek (~50 m),

142   as well as the presence of a berm located adjacent to the tidal creek (Seyfferth et., 2020; Hill et

143   al., 2021).

144

145   *2.2 Experimental set-up*

146   The experiment was performed over the course of 6 campaigns to cover a full growing

147   season: greenup (G), maturity (M), senescence (S), and dormancy (D) as described by the

148   canopy phenology of the study site (Hill et al., 2021). The campaigns began during the latter half

149   of the 2020 growing season and continued into beginning of the 2021 growing season ~~season~~

150   (M1 – 29 June to 2 July, M2 – 31 July to 3 Aug~~-~~, S1 – 31 Aug to 3 Sept, S2 – 28 Sept to 1 Oct,

151   D1 – 13 Apr to 16 Apr, and G1 – 31 May to 3 June) due to delays related to the COVID-19

152   pandemic. We installed six PVC collars (diameter: 20 cm), placed ~1.2 meters apart, four

153   months prior to the beginning of the experiment in the year 2020. Collars were placed in a *S.*

154   *alterniflora* area of the marsh near the boardwalk to minimize impacts to the marsh, as well as to

155   easily access boardwalk power outlets. Any vegetation that grew inside these collars in between

156   campaigns was carefully ~~removed~~clipped at the base of the stem prior to ~~the start of the~~

157 ~~measurements.~~each campaign. Vegetation was clipped on a frequent basis to minimize stem

158 diameters and thereby reduced the effects of plant-mediated gas transport. These collars were

159 used to set down six opaque automated chambers (LICOR 8100-104, Lincoln, Nebraska;

160 volume: 4071.1 cm^3) to measure trace gas fluxes as described below.

161

162 *2.3 Trace gas flux measurements and QA/QC*

163   The autochambers were coupled with a closed-path infrared gas analyzer (LI-8100A,

164 LICOR, Lincoln, Nebraska) and a Fourier transform infrared spectrometer (DX4040, Gasmet

165 Technologies Oy, Vantaa, Finland). The LI-8100A and the DX4040 were connected in parallel

166 since the DX4040 has its own internal pump and flow rates. Trace gas fluxes were measured

167 once per hour per chamber (i.e., all six chambers were measured within an hour). Measurements

168 were 5 minutes long and each chamber was flushed for 5 minutes total (pre-purge and post-purge

169 were both 2.5 minutes long) to help reduce the impacts of humidity on the instruments. Each

170 campaign lasted approximately 72 hours where approximately 416 measurements were recorded.

171 Campaigns were short in length due to electrical power limitations and to minimize

172 instrumentation damage due to the corrosive environmental conditions.

173   At the beginning of each campaign and every 24 hours after, we performed a zero

174 calibration on the DX4040 using ultra-pure 99.999% N$_2$ gas. It is recommended that zero

175 calibrations are performed every 24 hours and when the ambient temperature changes by 10°C,

176 so the experiment was paused for ~30 minutes during the zero calibrations each day. Gas fluxes

177 were calculated using Soil Flux Pro (v4.2.1, LICOR, Lincoln, Nebraska) and underwent

178 standardized quality assurance and quality control protocol as established in previous

179 publications (Capooci et al., 2019; Petrakis et al., 2017). ~~Briefly, QAQC~~QA/QC included

180 removingseveral steps. First, all values due to instrumental errors, comparing such as an

181 insufficient chamber closure seal were removed. These errors were identified by the SoilFluxPro

182 software. Second, the R^2 for the linear and exponential and linear fits to select for the

183 measurementof trace gas emissions were compared and the fit with the higher R^2, removing was

184 chosen. Third, all measurements during times wherefluxes that occurred when the R^2 forof CO_2

185 <was <0.90, and removing were removed. Low R^2's indicate that the soil micrometeorological

186 conditions were not stable during the measurement. Finally, all negative CO_2 fluxes. were

187 removed since they were likely erroneous.

188

189 *2.4 Ancillary measurements*

190   Meteorological (station: delsjmet-p) and water quality (station: Aspen Landing) data were

191 obtained from the National Estuarine Research Reserve's Centralized Data Management Office

192 (CDMO) and collected according to their protocol (System-wide Monitoring Program).

193 Meteorological data was collected using a CR1000 Meteorological Monitoring Station

194 (Campbell Scientific, Logan, UT, USA). Water quality data were measured using a YSI 6600

195 sonde (YSI Inc., OH, USA). Both data sets were cleaned and gap-filled following the protocol

196 established in Capooci et. al. (2022).

197

198 *2.4 Ancillary measurements*

199   Meteorological (station: delsjmet-p) and water quality (station: Aspen Landing) data were

200 obtained from the National Estuarine Research Reserve's Centralized Data Management Office

201 (CDMO) and collected according to their protocol (System-wide Monitoring Program).

202 Meteorological data was collected using a CR1000 Meteorological Monitoring Station

203 (Campbell Scientific, Logan, UT, USA). Water quality data were measured using a YSI 6600

204 sonde (YSI Inc., OH, USA). Both data sets were cleaned and gap-filled following the protocol

205 established in Capooci et. al. (2022).

206   Phenological data were obtained from the PhenoCam network (site: stjones,

207 Seyednasrollah et al., 2019) as described previously ~~(Trifunovic et al., 2020; Hill et al.,~~

208 ~~2021)~~(Trifunovic et al., 2020; Hill et al., 2021). Briefly, a single mid-day photo (12:00:00 h) was

209 selected for each of the days in the study period and was visually inspected to remove images

210 with obvious distortions. Since the images included a variety of vegetation types, the region of

211 interest delineated to only the area containing *S. alterniflora*, the main species at the study site.

212 Then the phenopix R package (Filippa et al., 2020) was used to extract and calculate the

213 greenness index, as well as delineate the phenophases for the study period (Hill et al., 2021).

214

215 *2.5 Data analyses*

216   Daily averages and associated standard deviations were calculated for meteorological and

217 water quality data, except for the greenness index. Soil trace flux data were averaged into hourly

218 and daily means and standard deviations. For heat maps, average hourly and campaign-length

219 coefficients of variation were calculated.

220   We extracted measurements from the time series of the automated measurements to

221 represent information collected from discrete temporal measurements conducted during daytime

222 low tide. This approach aimed to represent a measurement protocol derived from manual (i.e.,

223 survey) measurements where most measurements are performed at daytime and low tide for

224 logistical reasons. To identify and extract these measurements, we identified when low tide

225 occurred during each day (between 9:00:00 and 17:00:00 h) of the campaigns from water level

226   data obtained from the tidal creek. All automated measurements that fell between 1 hour before

227   and 1 hour after low tide were extracted, averaged into a daily value, and classified as "discrete"

228   measurements. For example, if low tide fell at 13:00:00 h, all continuous measurements that fell

229   between 12:00:00 and 14:00:00 h were then extracted and averaged to obtain a daily mean. Daily

230   means were also calculated for all automated measurements collected during the day and will be

231   referred to as the "continuous" daily mean. Differences in the means and distributions of the

232   continuous and discrete fluxes were assessed using a t-test and a Kolmogorov-Smirnov test,

233   respectively.

234   Sustained global warming potential (SGWP) was calculated for both the campaign-long

235   and daytime low tide fluxes for CO_2, CH_4, and N_2O. SGWP accounts for sustained gas emissions

236   over time compared to the global warming potential which accounts for a pulse emission over

237   time (Neubauer and Megonigal, 2019).(Neubauer and Megonigal, 2019). To calculate the

238   SGWP, data from Day 2 and 3 of each campaign was used since measurements on Day 1 and 4

239   did not always occur during daytime low tide. Fluxes were converted into g m^{-2} and multiplied

240   by the 20 and 100-year SGWP (Neubauer and Megonigal, 2019).(Neubauer and Megonigal,

241   2019). SGWP were compared to see whether extrapolating SGWP from daily-averaged manual

242   measurements done at low tide yielded similar values as hourly-averaged from high temporal

243   frequency measurements.

244

245   **3. Results**

246

247   *3.1 Meteorological and water quality*

11

248   Air temperature and greenness index show traditional seasonal patterns of temperate salt

249   marshes (Fig. 1). Daily mean air temperature ranged from -3.5°C to 29.9°C, with an average

250   daily temperature of 13.8 ± 9.1°C, while greenness index ranged from 0.30 to 0.42 with an

251   average of 0.34 ± 0.04. Relative humidity, barometric pressure, water level, and salinity varied

252   throughout the year. Relative humidity ranged from 32.6% to 100% with an average of $79.1\% \pm$

253   16.7%. Barometric pressure was between 999.7 and 1036 mb with an average value of $1018.3 \pm$

254   6.8 mb. Daily water level ranged from -0.30 m to 0.76 m with an average height of 0.25 ± 0.2 m,

255   while salinity ranged from 1.1 ppt to 20.4 ppt with an average of 8.0 ± 4.45 ppt.
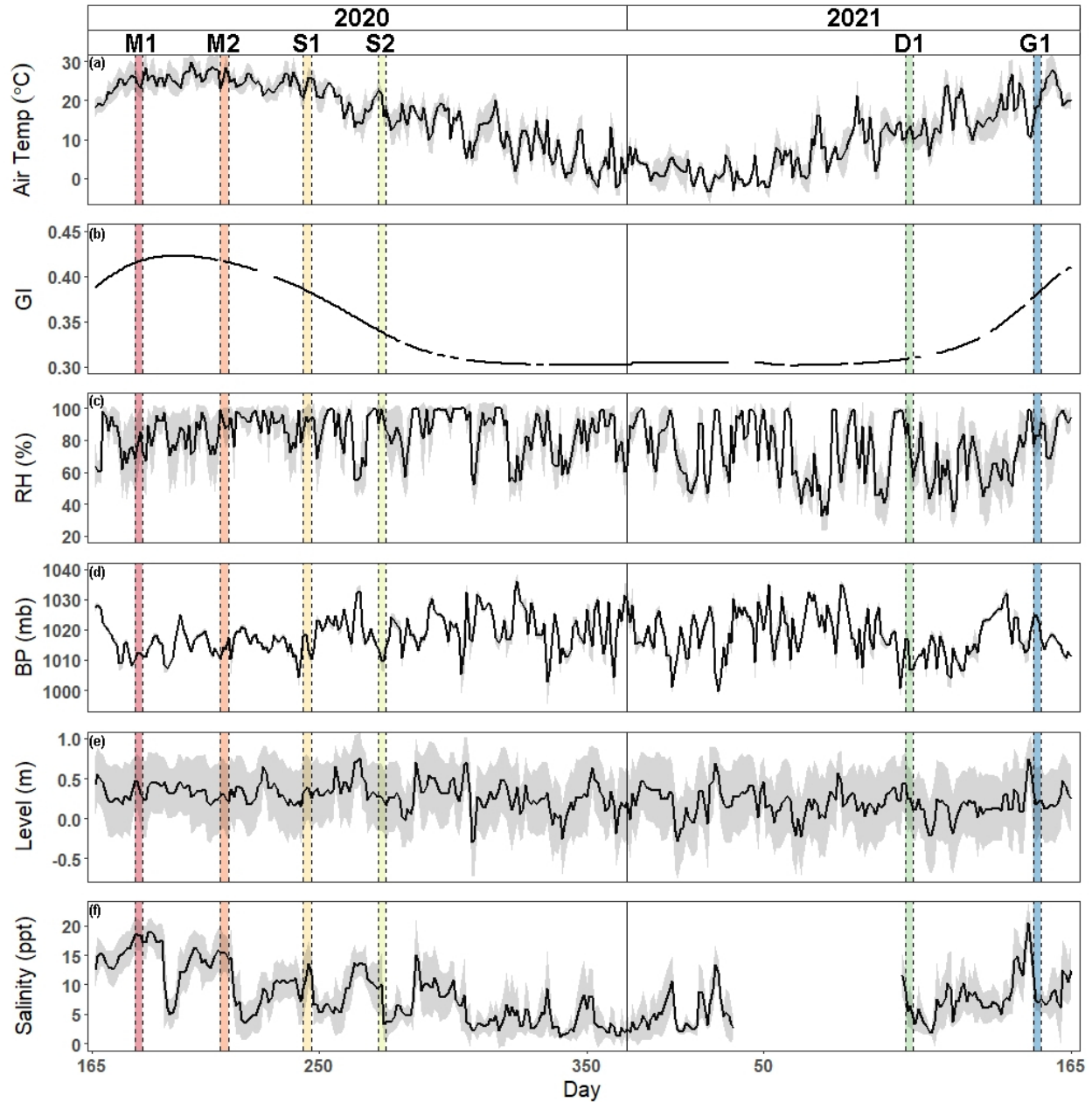
256

257

Figure 1. Time series of hourly mean ± SD (gray shaded region of (a) air temperature, (b)

greenness index, (c) relative humidity, (d) barometric pressure, (e) water level, and (f) salinity

from June 14, 2020 to June 14, 2021. Vertical shaded areas correspond to each of the campaigns

(M = maturity, S = senescence, D = dormancy, G = greenup).

262

263

264   *3.2 Greenhouse gas and sulfur-based trace gas patterns and variability*

265   Average CO_2 fluxes were significantly different in each campaign, with the highest

266   average fluxes occurring during the G1 campaign and the lowest during the D1 campaign (Fig.

267   2a). During some campaigns, such as S1, CO_2 fluxes did not show similar temporal patterns

268   between chambers, whereas during other campaigns, such as M2 and G1, all six chambers had

269   similar patterns. While there is a seasonal pattern in CO_2 fluxes, with higher fluxes occurring

270   during warmer months, diel patterns were not consistent between campaigns. One notable

271   exception is the G1 campaign, during which a clear diel pattern was observed. CO_2 fluxes had

272   consistent variability from one hour to the next during each of the 6 campaigns (Fig. 3a), with

273   overall average variability ranging from 28.9% during M2 to 49.6% during Dl.

274   CH_4 fluxes were low most of the time, particularly during the G1 campaign (Fig. 2b).

275   However, CH_4 pulses occurred during 5 out of the 6 campaigns, with S1and S2 having the most

276   frequent pulse emissions. S2 had the largest CH_4 pulse,13,488 nmol m^{-2} s^{-1}, which was 2,599%

277   higher than the average flux. The highest average CH_4 fluxes also occurred during S1 and S2,

278   while the highest hourly variability occurred in both S1 and S2, as well as in M2 (Fig. 3b). Mean

279   CH_4 variability ranged from -108% in M1 to 91.0% in S1.

280   Most N_2O fluxes were near-zero, with periodic pulses of emissions or uptake that ranged

281   from -33.8 to 19.0 nmol m^{-2} s^{-1} (Fig. 2c), with a maximum percent change from the mean of

282   10,231%. Four out of the six campaigns (M1, S2, D1, and G1) had net N_2O uptake, while two

283   campaigns (M2, S1) had net N_2O fluxes. There were no significant differences between

284   campaigns except for M1 and S1. Meanwhile, N_2O fluxes had very high hourly variability

285   ranging from -106,964% to 26,208% (Fig. 3c). Consequently, average variability during each

286   campaign was highly variable from -1,032% to 129%.

287   Similarly to CH_4 and N_2O, CS_2 fluxes were low the majority of the time, with occasional

288   pulses of emissions or uptake (Fig. 2d). CS_2 fluxes ranged from -386.9 to 306.2 nmol m^{-2} s^{-1},

289   with a maximum percent change from the mean of 4,785%. All campaigns had net emissions

290   despite periodic pulses of CS_2 uptake. CS_2 fluxes also had high hourly variability, with overall

291   means for each campaign ranging from -70.2% during D1 to 2254% during M2 (Fig. 3d).

292   DMS emissions were zero for most of the campaigns (Fig. 2e). Pulses of emissions and

293   uptake tended to occur during mid-day. DMS fluxes ranged from -158.5 to 230 nmol m^{-2} s^{-1},

294   with a maximum percent change from the mean of 185,987%. D1 and G1 had net uptake, while

295   the other four campaigns had net emissions of DMS. During periods of emissions and uptake,

296   hourly variability ranged from -870.5% to 888.7% (Fig. 2e). The extended periods of no DMS

297   fluxes contributed to low overall mean variability during each campaign, ranging from -2.45% in

298   S2 to 35.7% in M2.

299

300

16

Figure 2. Time series of fluxes from each chamber during each campaign for (a) CO_2, (b) CH_4, (c) N_2O, (d) CS_2, and (e) DMS. Each color designates a different chamber. The campaign means [LCI = lower 95% confidence interval, UCI = upper 95% confidence interval] are listed on each panel. The y-axis for CH_4 fluxes was shortened to show the variability. Full range of CH_4 fluxes during S2 can be seen in Supplementary Figure (SF) 1.
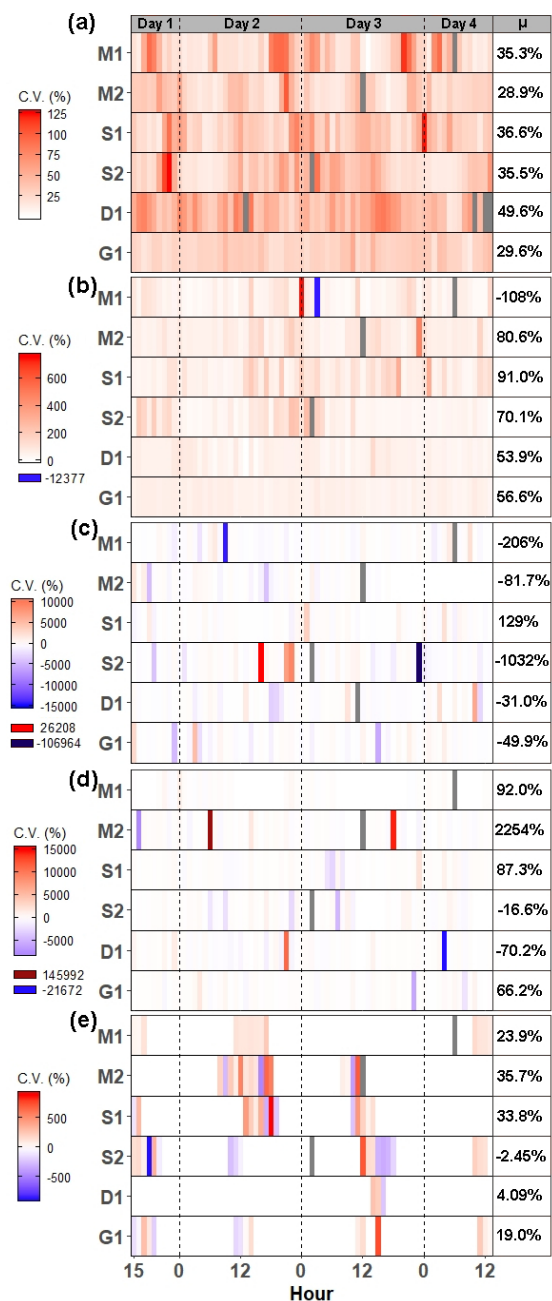
17

Figure 3. Heat maps of hourly coefficient of variance (CV) for (a) CO_2, (b) CH_4, (c) N_2O, (d) CS_2, and (e) DMS during each campaign. Each pixel represents the average CV for that hour. Mean CV for each campaign is listed in the μ column. Grayed out pixels represent NA. Note: legend scale is different for each gas and campaigns start at 15:00:00 h on Day 1 and end at 13:00:00 h on Day 4.

18

313   *3.3 Comparisons between continuous and discrete measurement scenarios*

314   A subset of the continuous measurements that fall during daytime low tide was selected

315   to represent data collected using traditional discrete, manual measurements which are commonly

316   reported for tidal salt marshes. Information from continuous and discrete datasets are compared

317   to elevate whether they provide similar distributions, daily means, flux-temperature

318   relationships, and SGWP.

319   Continuous and discrete flux distributions can be seen via density plots (Fig. 4). While

320   the distributions for continuous and discrete fluxes overlap for each of the five gases, four of the

321   five gases have significantly different distributions of fluxes when comparing the continuous and

322   the discrete datasets (Table 1). The only gas that had similar distributions between the two

323   sampling intervals was CO_2 (Table 1). For all gases, the continuous distribution had higher

324   kurtosis values and higher C.V. than the discrete fluxes (Table 1). Of the five gases, CS_2 was the

325   only one with a more skewed discrete data distribution and significantly different means between

326   continuous and discrete measurement scenarios (Fig. 4b, Table 1).

327   For CS_2 and DMS, discrete measurements had higher overall daily mean fluxes (Fig. 5d,

328   5e), while the opposite occurred for CH_4 and N_2O (Fig. 5b, 5c). CO_2 fluxes from continuous and

329   discrete measurements had nearly a 1:1 relationship (Fig. 5a). Both CO_2 and DMS had strong

330   relationships between continuous and discrete daily means, with r-squares higher than 0.7, while

331   N_2O and CS_2 had moderate relationships. CH_4 had a poor fit between continuous and discrete

332   measurements.

333   Next, relationships between trace gas flux and air temperature were evaluated for each

334   gas under continuous and discrete measurement scenarios. CO_2 and CH_4 fluxes had statistically

335   significant relationships for both discrete and continuous measurements versus air temperature

19

336   (Fig. 6a-d). Air temperature explained 38% and 21% of the variability for discrete and

337   continuous measurements for CO_2, respectively (Fig. 6a, b), while air temperature explained

338   32% and 7% of the variability for discrete and continuous measurement for CH_4 (Figs. 6c, d).

339   The slopes for both discrete and continuous CO_2 fluxes were not significantly different (95% CI;

340   0.029 - 0.12, 0.037 - 0.054, respectively), as well as for CH_4 (95% CI; 2.14 - 12.7, 1.31 - 2.71,

341   respectively). For N_2O, CS_2, and DMS, there were no significant relationships between discrete

342   daily mean fluxes and air temperature, but there were significant relationships between

343   continuous hourly mean fluxes and air temperature (Fig. 6e-j). Air temperature explained very

344   little variability for N_2O, CS_2, and DMS.

345   Discrete measurements had a higher SGWP potential than the continuous measurements.

346   (Table 2). While the discrete measurements had a slightly lower SGWP for CO_2 and a slightly

347   higher SWGP for N_2O, the difference between continuous and discrete SGWP was driven by

348   CH_4. The 20-yr and 100-yr SGWP for discrete measurements of CH_4 were up to ~38% higher

349   than the respective continuous measurements, contributing to an overall increase of ~18% and

350   ~11% for the discrete measurement's 20- and 100-year SGWP.

351
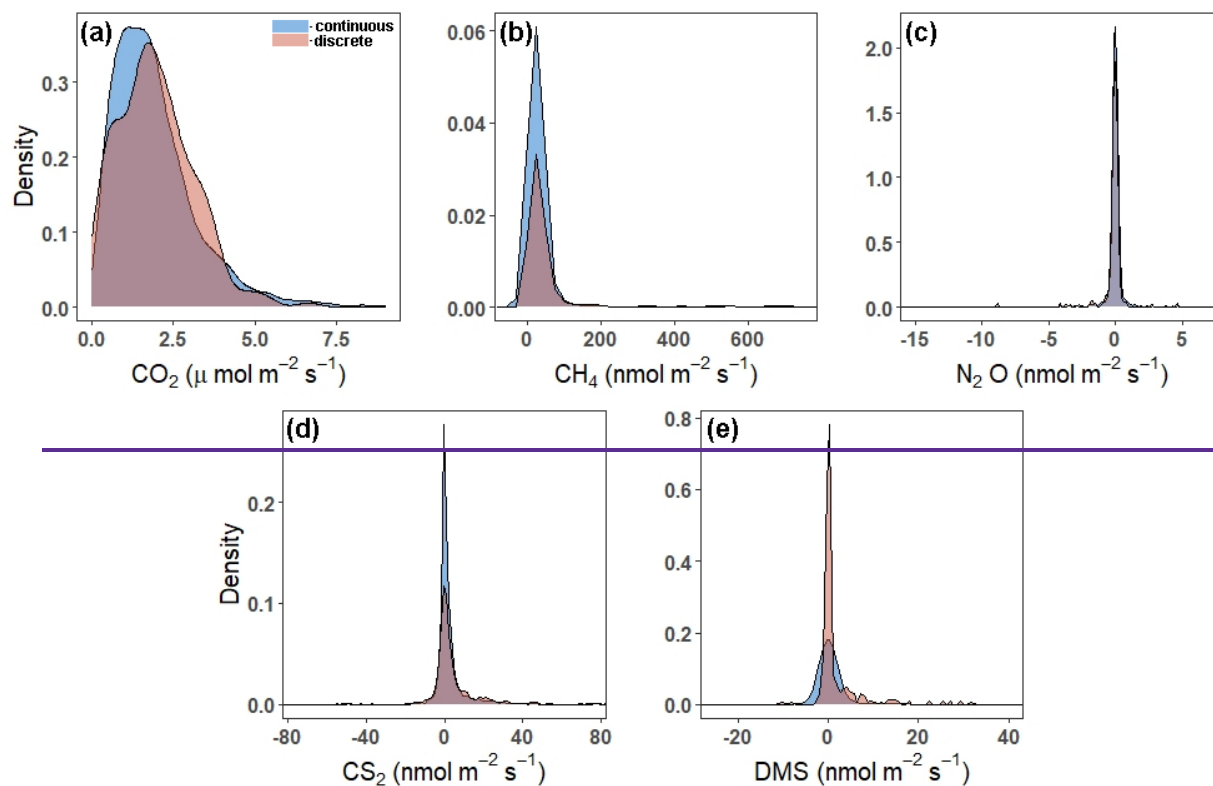
352
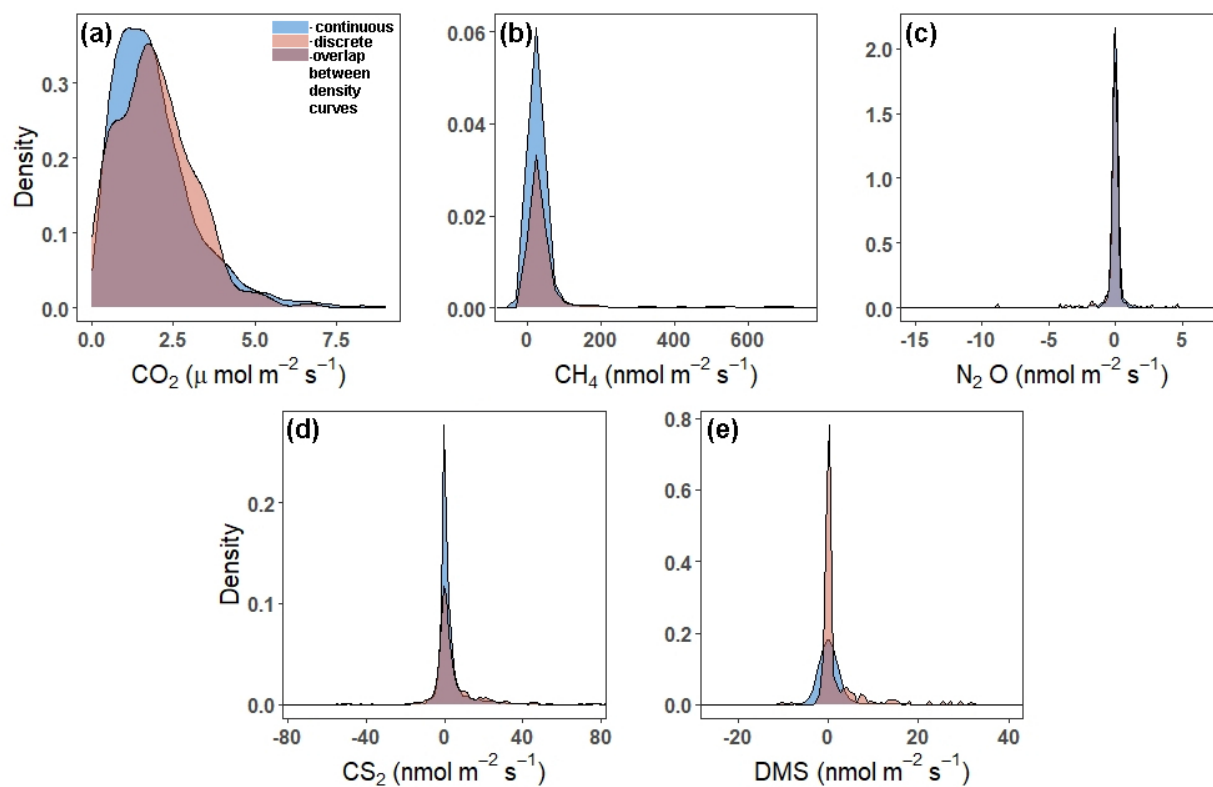
353

354 **Figure 4.** Density plots comparing the distribution of fluxes throughout all campaigns

355 (continuous over ~72 hours) to those measured during daytime low tide (discrete, one hour

356 before and one hour after daytime low tide) for (a) CO_2, (b) CH_4, (c) N_2O, (d) CS_2, and (e) DMS.

357 Note: The scales on the x- and y-axes are different. The tails have been cut off to better see the

358 peaks for (b), (c), (d), and (e). To see plots with full distributions, see SF 2.

359 **Table 1.** Summary of continuous (over ~72 hours) and discrete (one hour before and one hour

360 after low tide) measurement data and distributions for each gas. An alpha of < 0.05 was used to

361 determine significant differences between the means and the distributions. Note: Means for CO_2

362 are in $\mu mol\ m^{-2}\ s^{-1}$, while the other gases are in $nmol\ m^{-2}\ s^{-1}$.

363

| Gas	Sampling Frequency	Mean	95% CI	C.V.	Skewness	Kurtosis	Means Different?	Distributions Different?
CO_2	Continuous	1.92	1.86–1.97	67.2%	1.53	6.51	No	No
	Discrete	1.90	1.74–2.07	62.3%	0.67	3.65		
CH_4	Continuous	41.2	29.5–52.9	708%	41.6	1903	No	Yes p = 0.02
	Discrete	57.6	39.2–76.0	234%	5.21	34		
N_2O	Continuous	-0.06	-0.13–0.009	2686%	-4.67	133	No	Yes p < 0.001
	Discrete	-0.16	-0.29–-0.04	556%	-4.39	47.8		
CS_2	Continuous	3.39	2.45–4.33	673%	1.51	116	Yes p = 0.04	Yes p = 0.05
	Discrete	6.44	3.70–9.18	312%	3.93	22.9		
DMS	Continuous	1.11	0.70–1.51	907%	8.74	223	No	Yes p < 0.001
	Discrete	1.77	1.06–2.48	295%	3.40	16.6		

364

365

366
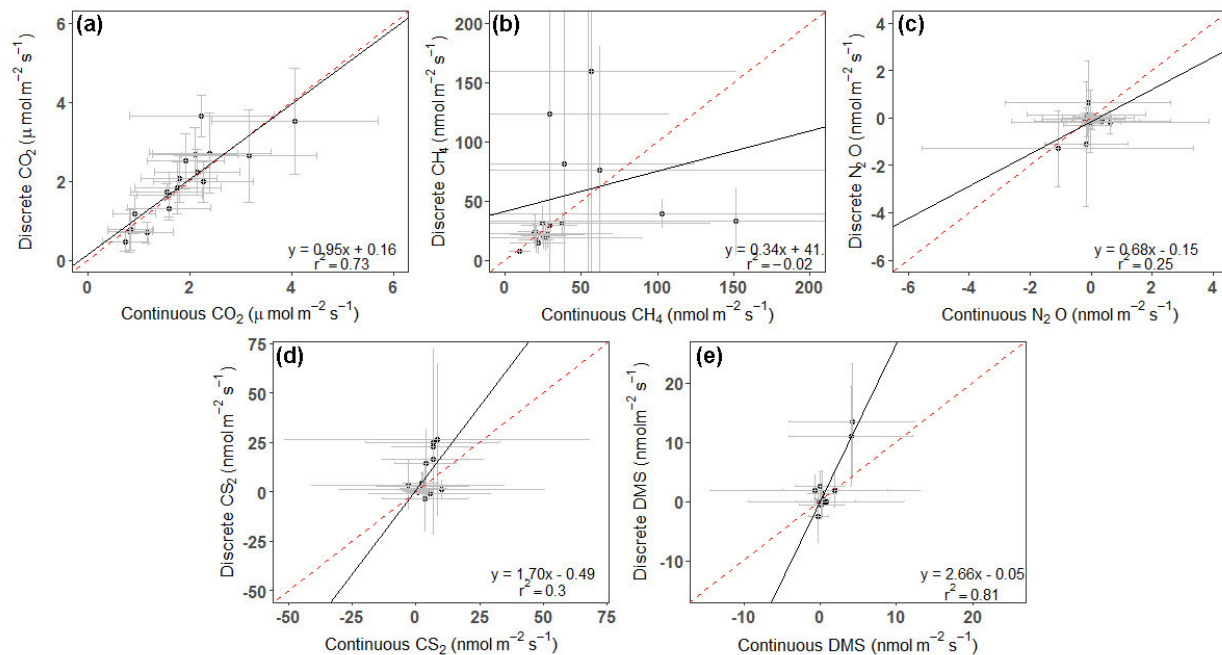
Figure 5. Plots comparing the daily average of continuous <u>(over ~72 hours)</u> to discrete <u>(one hour before and one hour after daytime low tide)</u> measurements for (a) CO_2, (b) CH_4, (c) N_2O, (d) CS_2, and (e) DMS. Error bars represent the SD and have been cut off in panel (b) to show data better. See SF 3 for full error bars for panel b. Red dashed line is the 1:1 line, while the black solid line is the trend line.
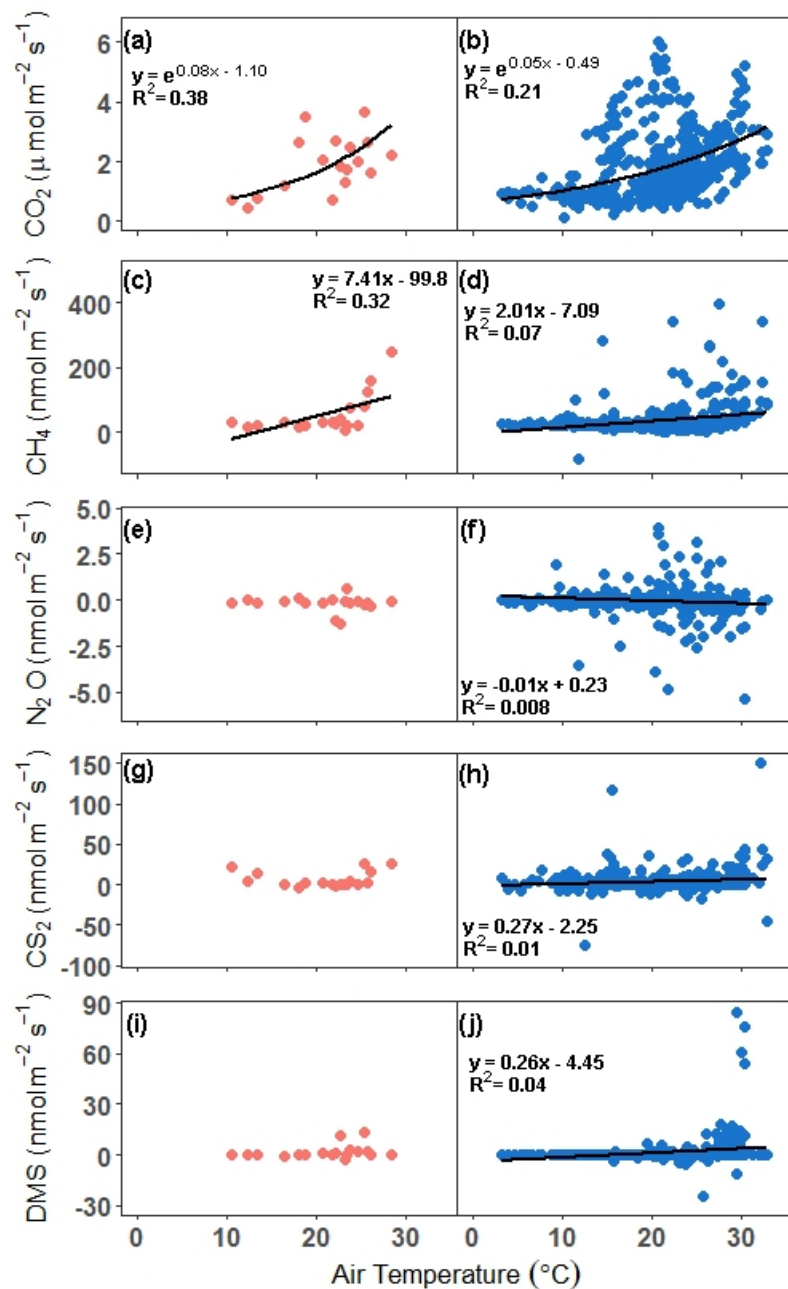
Figure 6. Comparison of fluxes versus air temperature for all campaigns. In panels, a, c, e, g, and I, the hourly continuous (over ~72 hours) mean is compared to the hourly air temperature, while in panels b, d, f, h, and k, the discrete (one hour before and one hour after daytime low tide) daily mean is compared to the daily air temperature. The trend lines for significant relationships at

377 alpha <0.05 are plotted. Note: In panel d, the outlier hourly mean of 2,275 nmol m^{-2} s^{-1} is not

378 included in the trend line or in the graph.

379

380 **Table 2.** Sustained global warming potential (SGWP) derived from continuous (over ~72 hours)

381 and discrete ~~temporal (during~~(one hour before and one hour after daytime low tide) temporal

382 measurements in a tidal salt marsh.

383

Frequency	CO$_2$ (g m^{-2})	CH$_4$ (CO$_{2\text{-eq}}$ (g m^{-2}))		N$_2$O (CO$_{2\text{-eq}}$ (g m^{-2}))		Total (CO$_{2\text{-eq}}$ (g m^{-2}))	
		20-yr SGWP	100-yr SGWP	20-yr SGWP	100-yr SGWP	20-yr SGWP	100-yr SGWP
Continuous	84.9	70.4	33.0	0.27	0.30	155.57	118.2
Discrete	82.7	103.2	48.4	0.40	0.44	186.3	131.54

384

385

386 **4. Discussion**

387 *4.1 Measuring all the time: seasonal and diel patterns and hot moments of soil trace gases*

388   Spatial variability between the individual chambers at SS were low, but CO$_2$ fluxes

389 showed temporal variability that corresponded to changes in temperature. The relatively low

390 spatial variability within our experimental setting contrasts with previously reported high spatial

391 variability of CO$_2$ fluxes attributed to the presence of a hot spot ~~(Capooci and Vargas,~~

392 ~~2022).~~(Capooci and Vargas, 2022). However, previous CO$_2$ fluxes measured at the SS site

393 ranged from 0-~~10~~15 μmol m^{-2} s^{-1}, with the bulk of the measurements between 0-~~4~~5 μmol m^{-2} s^{-1},

394 with higher fluxes associated with hot spots or warmer temperatures ~~(Capooci and Vargas, 2022;~~

395 ~~Seyfferth et al., 2020).~~(Capooci and Vargas, 2022; Seyfferth et al., 2020; Hill and Vargas, 2022).

396   Therefore, location of measurements within a landscape could be influenced by hot spots, which

397   complicates ecosystem scale calculations of soil CO_2 fluxes (Barba et al., 2018). In addition,

398   there was a seasonal pattern evident in the CO_2 fluxes, with higher emissions during the growing

399   season, as typical in temperate ecosystems, as well in the significant relationship between CO_2

400   and air temperature. ~~Other studies at temperate wetland sites have found higher fluxes during the~~

401   ~~summer (Simpson et al., 2019; Yu et al., 2019; Bridgham and Richardson, 1992)~~Within salt

402   marshes, soil organic matter decomposition into products such as CO_2 correlates with

403   temperature due to the activation energy needed for organic matter breakdown (McTigue et al.,

404   2021). Other studies at temperate wetland sites have found higher fluxes during the summer

405   (Simpson et al., 2019; Yu et al., 2019; Bridgham and Richardson, 1992), as well as relationships

406   between CO_2 fluxes and temperature ~~(Capooci and Vargas, 2022; Simpson et al., 2019; Xie et~~

407   ~~al., 2014)~~(Capooci and Vargas, 2022; Simpson et al., 2019; Xie et al., 2014) highlighting that

408   CO_2 fluxes in temperate salt marshes exhibit a temperature dependency over seasonal scales,

409   even in the presence of tides.

410   While CO_2 fluxes show seasonal patterns, there are no diel patterns that persist

411   throughout the year. During G1, the peak of high tide coincided with peak daily temperature.

412   This scenario also occurred during D1, but fluxes were too low to discern patterns. During all

413   other campaigns, low tide and peak temperatures coincided. These results suggest that diel

414   patterns may occur periodically under certain conditions. For example, at the SS site, it may be

415   that diel patterns occur during high tide at the temperature peak. While we expected the highest

416   fluxes during low tides due to increased oxygen exposure, there may be a lag between low tide in

417   the creek and low water levels at the SS site, resulting in higher fluxes during high tide in the

418   creek. However, these results can vary from site to site and with proximity to the tidal creek.

27

419 More research using high temporal frequency measurements are needed to parse out the role of

420 temperature and tides on CO_2 fluxes across salt marshes to properly represent the pattern in earth

421 system models (Ward et al., 2020)

422 ~~Similarly to CO_2, CH_4 has a significant relationship with air temperature, however it~~

423 ~~explains less variability in the fluxes. Several studies have found positive correlations between~~

424 ~~soil CH_4 fluxes and temperature (Bartlett et al., 1985; Emery and Fulweiler, 2014; Wang and~~

425 ~~Wang, 2017) in temperate salt marshes, while others have not~~ Similarly to CO_2, CH_4 has a

426 significant relationship with air temperature, however it explains less variability in the fluxes.

427 Several studies have found positive correlations between soil CH_4 fluxes and temperature

428 (Bartlett et al., 1985; Emery and Fulweiler, 2014; Wang and Wang, 2017) in temperate salt

429 marshes, while others have not (Wilson et al., 2015)~~. It is important to note that while, in general,~~

430 ~~salt marsh CH_4 fluxes are positively related to temperature (Al-Haj and Fulweiler, 2020), the~~

431 ~~ability of temperature to explain CH_4 flux variability is low, compounded by many, often site-~~

432 ~~specific, factors that affect methane production and consumption, such as organic matter supply,~~

433 ~~microbial communities, and diffusion rates (Al-Haj and Fulweiler, 2020; Bartlett et al., 1985).~~

434 ~~At our study site, CH_4 fluxes were highest and pulses were most frequent during senescence,~~

435 ~~agreeing with findings from ecosystem-scale measurements derived using the eddy covariance~~

436 ~~technique (Vázquez-Lule and Vargas, 2021).~~. It is important to note that while, in general, salt

437 marsh CH_4 fluxes are positively related to temperature (Al-Haj and Fulweiler, 2020), the ability

438 of temperature to explain CH_4 flux variability is low, compounded by many, often site-specific,

439 factors that affect methane production and consumption, such as organic matter supply,

440 microbial communities, and diffusion rates (Al-Haj and Fulweiler, 2020; Bartlett et al., 1985).

441   At our study site, CH_4 fluxes were highest and pulses were most frequent during

442   senescence, agreeing with findings from ecosystem-scale measurements derived using the eddy

443   covariance technique (Vázquez-Lule and Vargas, 2021). In most wetland ecosystems, including

444   those in northern, temperate, and subtropical areas, the highest fluxes have been reported during

445   the summer ~~(Kim et al., 1998; Rinne et al., 2007; Van Der Nat and Middelburg, 2000; Livesley~~

446   ~~and Andrusiak, 2012)~~(Kim et al., 1998; Rinne et al., 2007; Van Der Nat and Middelburg, 2000;

447   Livesley and Andrusiak, 2012; Turetsky et al., 2014), but we highlight that there is a lack of

448   measurements during the winter ~~(Al-Haj and Fulweiler, 2020).~~(Al-Haj and Fulweiler, 2020).

449   In *S. alterniflora* marshes, highest mean CH_4 fluxes have been found in both the summer and the

450   fall ~~(Bartlett et al., 1985; Emery and Fulweiler, 2014)~~(Bartlett et al., 1985; Emery and Fulweiler,

451   2014). At a site dominated by *S. alterniflora,* both high fluxes and porewater CH_4 concentrations

452   were found in September~~, indicating either a continual build-up of CH_4 in the pore water over the~~

453   ~~growing season and/or increased CH_4 production in the fall.~~ (Zhang and Ding, 2011), indicating

454   either a continual build-up of CH_4 in the porewater over the growing season and/or increased

455   CH_4 production in the fall. For our site, it is likely higher CH_4 emissions during senescence were

456   due to an input of labile organic matter from plant die-off (Seyfferth et al., 2020). Furthermore, a

457   recent study has shown that porewater DMS, a non-competitive substrate for methylotrophic

458   methanogenesis that is produced from the breakdown of DMSP, a metabolite produced by *S.*

459   *alterniflora* (Dacey et al., 1987), peaks during the fall (Tong et al., 2018). Therefore, we

460   postulate that an influx of DMS may also contribute to higher CH_4 fluxes during senescence in

461   marshes dominated by *S. alterniflora*. This finding highlights the importance of carbon-sulfur

462   biogeochemistry and measuring fluxes during non-summer months; particularly in marshes that

463   have plant communities that provide substrates used in methylotrophic methanogenesis

464   (Seyfferth et al., 2020).

465   On a diel timescale, pulse emissions of CH_4 from the soil tend to occur during the

466   warmest time of the day, as well as during low and rising tides. There are very few studies that

467   report high-temporal frequency data of CH_4 emissions, most of which include plants within their

468   scope (via transparent chambers or eddy covariance) or focus on tidal creeks, making it difficult

469   to ascertain whether the diel patterns seen in this study are typical of tidal salt marsh soils.

470   ~~Considering~~Of the ~~broader range of~~ studies ~~about~~that report high-temporal frequency data of

471   plant or water-based CH_4 fluxes in coastal vegetated ecosystems, CH_4 emissions have been

472   found to peak at various points in the day, from during the day ~~(Yang et al., 2018, 2017; Tong et~~

473   ~~al., 2013)~~(Yang et al., 2018, 2017; Tong et al., 2013), at night (Diefenderfer et al., 2018), or

474   highly variable (Jha et al., 2014; Xu et al., 2017). At our site, CH_4 fluxes tended to peak at the

475   confluence of peak daily temperature and low to rising tides, indicating that physical forcing may

476   contribute to CH_4 pulses ~~(Bahlmann et al., 2015; Middelburg et al., 1996)~~(Bahlmann et al., 2015;

477   Middelburg et al., 1996). However, pulses did occur during other times throughout the day and

478   within the tidal cycle. While some of the pulse emissions may be a result of ebullition, the

479   majority are associated with high R^2's, indicating that they are sustained over the measurement

480   period. Our results demonstrate the importance of conducting high-temporal frequency CH_4

481   measurements in tidal salt marsh soils for several reasons, including the need for more data to

482   better understand the drivers of CH_4 fluxes at diel scales and how that affects model predictions.

483   N_2O emissions and uptake loosely followed a seasonal pattern, likely driven by the

484   canopy phenological stages. During the growing season, it has been shown that highly

485   productive plants can compete with soil microbes for NO_3^- and NH_4^- ~~(Cheng et al., 2007; Yu et~~

al., 2012; Zhang et al., 2013; Granville et al., 2021; Xu et al., 2017)(Cheng et al., 2007; Yu et al.,

2012; Zhang et al., 2013; Granville et al., 2021; Xu et al., 2017), shifting denitrifiers into

consuming N_2O and resulting in a net uptake during G1 and M1. As the plants reach peak

maturity, the system shifts into net emission of N_2O during M2 and S1. One study found that

nitrogen additions resulted in a pulse of N_2O in July when most of the plant growth had occurred,

but no response in April, suggesting that the competition for NO_3^- and NH_3^+ decreases when

plant growth has slowed down (Moseman-Valtierra et al., 2011). Increased substrate availability

combined with warm temperatures likely contributed to the marsh being a net source of N_2O

during the later stages of the growing season. As temperatures drop, the system shifts back into

net uptake, as seen during S2 and D1. Similar seasonal patterns have been seen in other studies,

albeit shifted by a month or two depending on the local climate and phenophases (Granville et

al., 2021; Emery and Fulweiler, 2014)(Granville et al., 2021; Emery and Fulweiler, 2014). These

findings highlight balance between processes that produce N_2O (e.g., nitrification,

denitrification, and nitrifier-denitrification) and consume N_2O (e.g., denitrification), as well as

substrate availability and plant phenology in determining whether a marsh is a source or sink of

N_2O at any given point.

As with seasonality, diel patterns of N_2O showed both emissions and uptake. Several

studies have also reported both emissions and uptake during a 24-hour period (Yang et al., 2017;

Tong et al., 2013)(Yang et al., 2017; Tong et al., 2013). We found that pulses of uptake and

emissions occurred both during the day and at night, as well as during different phases of the

tidal cycle. Studies have found higher fluxes during the day (Tong et al., 2013; Yang et al., 2017)

and at night (Laursen and Seitzinger, 2002; Yang et al., 2017; Bauza et al., 2002)(Laursen and

Seitzinger, 2002; Yang et al., 2017; Bauza et al., 2002). Generally, fluxes were slightly higher at

509 night throughout the campaigns, perhaps as a result of increased availability of NH_4^+ at night due

510 decreased competition from photosynthesizers (Bauza et al., 2002). Overall, N_2O fluxes were

511 near-zero with a < 0.50 nmol m^{-2} s^{-1} difference between daytime and nighttime mean fluxes,

512 suggesting that N_2O fluxes do not play a major role in GHG emissions at this salt marsh.

513   Our automated measurements of sulfur-based trace gases show high variability in CS_2,

514 with low fluxes punctuated by occasional pulse emissions. There are no previous studies with

515 automated measurements to compare our findings, but previous studies have noted that CS_2

516 fluxes are highly variable ~~(Steudler and Peterson, 1985; Hines, 1996), with periods of emission~~

517 ~~and uptake.~~(Steudler and Peterson, 1985; Hines, 1996), with periods of emission and uptake.

518 However, fluxes at SS were, on average, an order of magnitude higher than values reported in

519 the literature (Supplementary Table 1). There could be several reasons for the difference in

520 magnitudes: 1) improvement in instrumentation to detect CS_2, 2.) sampling technique

521 differences, and 3.) site-specific characteristics. Since the influx of sulfur-based trace gas

522 measurements in the 1980s, instrumentation has advanced from using molecular sieves and

523 cryotraps to store samples before measuring them on a gas chromatograph (e.g., ~~Carroll et al.,~~

524 ~~1986; Cooper et al., 1987; Steudler and Peterson, 1984)~~Carroll et al., 1986; Cooper et al., 1987;

525 Steudler and Peterson, 1984) to using portable Fourier transform infrared (FTIR) spectrometers

526 that measure trace gas concentrations in near real-time. These instrumentation advances

527 subsequently led to changes in sampling techniques. Traditionally, it was common to keep the

528 chamber closed for upwards of 24-hours, with samples being collected over hourly intervals

529 throughout the day (Carroll et al., 1986; Goldan et al., 1987). Sweep air free of sulfur trace gases

530 was also commonly used to avoid the need to take samples at both the inlet and outlets of the

531 chambers (Goldan et al., 1987). However, others used ambient air because it more closely

532 resembled *in situ* conditions ~~(Steudler and Peterson, 1985).~~(Steudler and Peterson, 1985). With

533 recent advances, sampling techniques have changed to eliminate the need for very long closure

534 times and reduce the effects the chambers have on micrometeorological conditions. Now, high-

535 temporal frequency, long-term data can be obtained, thereby capturing pulse emissions that

536 otherwise may be missed. The third reason for difference in magnitude could be due to site-

537 specific differences in CS_2 fluxes. While the mechanisms by which CS_2 is produced are poorly

538 understood, there are several potential production pathways: OM degradation, photochemical

539 production, and algal production ~~(Xie and Moore, 1999).~~(Xie and Moore, 1999). The most likely

540 pathway for our site is the microbially-mediated reaction between H_2S and organic matter due to

541 high sulfur concentrations, anaerobic conditions, and a large pool of decaying organic matter.

542 Finally, CS_2 is a short-lived sulfur gas but the major product of CS_2 oxidation is COS;

543 consequently, understanding CS_2 production and oxidation is important for recognizing the role

544 of salt marshes in COS dynamics (Whelan et al., 2013).

545   The mean of measured DMS fluxes generally fall within those reported in the literature,

546 but with pulses higher than previously reported and different temporal patterns. We found that

547 DMS fluxes only occurred during the middle of the day, near when air temperatures peaked. This

548 is contrary to several studies that have found DMS fluxes during other times of the day

549 ~~(Morrison and Hines, 1990; Steudler and Peterson, 1985; DeLaune et al., 2002)~~(Morrison and

550 Hines, 1990; Steudler and Peterson, 1985; DeLaune et al., 2002). Some studies have found diel

551 patterns related to temperature ~~(De Mello et al., 1987; Cooper et al., 1987b)~~(De Mello et al.,

552 1987; Cooper et al., 1987b) and incoming tides ~~(Morrison and Hines, 1990; Dacey et al., 1987;~~

553 ~~Goldan et al., 1987)~~(Morrison and Hines, 1990; Dacey et al., 1987; Goldan et al., 1987). Our

554 results indicate that DMS fluxes from the SS site are associated with temperature and light-

555   related processes, whether these variables influence microbial activity, plant physiology, or a

556   combination of both. A study found that DMS fluxes peaked after a full daylight period in a

557   Danish estuary ~~(Jørgensen and Okholm-Hansen, 1985).~~(Jørgensen and Okholm-Hansen, 1985).

558   However, there is no information on the diel patterns of DMS in the sediment pore water or its

559   release from *S. alterniflora* plants. DMS is also produced by other pathways that occur under

560   anoxic conditions, such as methylation of sulfide and methanethiol (Lomans et al., 2002; Sela-

561   Adler et al., 2015), microbial reduction of dimethylsulfoxide ~~(Capone and Kiene, 1988)~~(Capone

562   and Kiene, 1988), and/or the incorporation of inorganic substrates (i.e., CO_2) and organic

563   methylated compounds ~~(Finster et al., 1990; Moran et al., 2008; Lin et al., 2010)~~(Finster et al.,

564   1990; Moran et al., 2008; Lin et al., 2010). To better understand DMS fluxes, more research into

565   the dynamics between *S. alterniflora*, pore water DMS, and DMS fluxes is needed, as it plays an

566   important role in carbon-sulfur biogeochemistry, particularly as a non-competitive substrate for

567   methylotrophic methanogenesis (Seyfferth et al., 2020) .

568

569   *4.2 Continuous versus discrete measurements: do we get the same information?*

570   Our results show that discrete temporal measurements of CO_2 during daytime low tide

571   throughout the year (including dormancy) may be sufficient to obtain a representative mean of

572   the temporal variability of soil CO_2 flux. This has implications for calculating carbon budgets.

573   Furthermore, the distribution of continuous and discrete CO_2 fluxes is similar, indicating that

574   discrete measurements are capturing similar variability as continuous measurements. This

575   observation is reinforced by the CO_2 ~ air temperature relationships, which do not have

576   significantly different slopes (discrete: 0.03 - 0.12, continuous: 0.04 - 0.05), providing further

577 support for the utility of daytime low tide discrete measurements in evaluating potential drivers

578 of CO_2 variability.

579 In contrast, high variability in CH_4 fluxes resulted in the means for discrete and

580 continuous measurements to be similar, but with significantly different distributions. In salt

581 marshes, CH_4 fluxes are characterized by high variability (Rosentreter et al., 2021), making it

582 difficult to assess the processes that control CH_4 fluxes ~~(Vázquez-Lule and Vargas,~~

583 ~~2021).~~(Vázquez-Lule and Vargas, 2021). While the means were not significantly different

584 despite ~33% higher mean flux using discrete measurements, it is important to note that the 95%

585 confidence interval and the coefficient of variation are broad and very high, resulting in potential

586 error cancellation for the calculation of the mean. We postulate that the discrete measurement

587 approach can be used to calculate budgets with the caveat of large uncertainties and that they

588 likely overestimate the mean CH_4 flux. Discrete measurements do not capture similar variability

589 as the continuous measurements and have a stronger air temperature-CH_4 flux relationship than

590 continuous measurements, despite the overlap between their confidence intervals (2.14 - 12.7

591 and 1.31 - 2.71, respectively). However, continuous measurements provide a more accurate

592 depiction of the patterns and magnitudes of CH_4 and can provide stronger insights into the

593 interrelated drivers of CH_4 fluxes.

594 Regardless of the sampling interval, N_2O fluxes had means that are near-zero. Due to

595 fluxes consistently being near zero, the discrete and continuous measurements will likely get

596 similar overall results due to error cancellation even if the distributions were significantly

597 different. The continuous measurements capture a wider range of fluxes than the discrete

598 measurements, as seen with its very high coefficient of variance and a different distribution.

599 However, the skewness between the two approaches is very similar, due to the bulk of the

600   measurements falling around the same values. as seen in the large amount of overlap in the

601   density curves. It is important to note that this site is nitrogen-limited, which constrains N_2O

602   production. In marshes that are not nitrogen-limited, sampling intervals will likely play a more

603   important role since fluxes will be higher.

604   For CS_2, discrete and continuous measurements did not have similar means or

605   distributions, likely due to the high variability found in these measurements. Previous studies

606   using discrete measurements of CS_2 have noted its high variability (e.g. De Mello et al., 1987),

607   with one highlighting the need for frequent measurements of sulfur-based trace gases during the

608   day in order to obtain an accurate mean daily flux value (Steudler and Peterson, 1985).(Steudler

609   and Peterson, 1985). We found that discrete measurements taken during daytime low tide result

610   in a daily mean that is nearly twice that of the daily mean from the continuous measurements.

611   The average CS_2 fluxes measured during our field campaigns were up to an order of magnitude

612   higher than previously reported. We advocate for more measurements of CS_2 fluxes beyond

613   focusing on low tide windows and during different canopy phenological phases across salt

614   marshes to better understand the dynamics of this trace gas.

615   When measuring DMS fluxes during daytime low tide, the mean is similar to the

616   continuous measurement mean, but the distributions are significantly different. However, caution

617   should be taken in using discrete measurements of DMS to calculate daily means, particularly if

618   those measurements fall during the warmest part of the day when DMS fluxes are the most

619   active. This could result in overestimating the daily mean since extended periods of no fluxes are

620   not accounted for. One approach to measuring DMS fluxes would be to use the strong

621   relationship between discrete and continuous measurements to correct for the overestimation of

622   discrete fluxes. However, this approach would still require the use of a continuous, automated

623 system at different points throughout the year to establish a site-specific correction of discrete

624 mean DMS fluxes, particularly if DMS fluxes are used to calculate DMS budgets.

625

626 **5. Conclusion: what are we missing: potential caveats? and challenges**

627   Discrete measurements have the clear advantage of capturing the spatial variability of soil

628 trace gas fluxes across an ecosystem, but this approach is also used to describe the temporal

629 variability. In contrast, continuous measurements using autochambers accurately describe

630 temporal patters (e.g., hourly measurements) but have limited spatial representation due to high

631 instrumentation costs and limited spatial extent of the area where autochambers can be deployed

632 (Vargas et al., 2011; Barba et al., 2018). Here we discuss the advantages and differences from

633 discrete and continuous measurements derived from this study. Discrete measurement campaigns

634 are suitable for calculating budgets, particularly for CO_2 and N_2O since they capture very similar

635 means. but not the temporal variability. While we found that CH_4 and DMS means were not

636 significantly different between the two approaches, there are caveats that must be considered

637 when using discrete measurements. The high variability inherent in CH_4 fluxes can contribute to

638 the lack of significant differences between the two approaches and result in discrete

639 measurements overestimating the overall CH_4 fluxes from a tidal salt marsh. This has

640 implications when calculating SWGP where differences in CH_4 means largely contribute to the

641 differences in SGWP between the two approaches and can affect how scientists and

642 policymakers view tidal salt marshes and blue carbon as a natural climate solution (Macreadie et

643 al., 2021). For DMS, it is important to assess diel patterns to ensure that fluxes are

644 representative, particularly at sites that have patterns similar to what is seen at our study site.

645 When evaluating variability or trying to parse out the processes that drive GHG and trace gas

646 emissions from tidal salt marshes, using continuous, automated measurements would be the best

647 approach. This is particularly important for CH$_4$, where pulse emissions are frequent during the

648 growing season and can be very high. Using continuous measurements is also important in

649 scenarios where discrete measurements do not capture a similar mean or distribution, as with CS$_2$

650 fluxes. However, discrete measurements are more capable of representing spatial variability, and

651 until we have a better understanding of which source of variability is higher, temporal~~,~~ or spatial,

652 both techniques should be considered for ecosystem assessments.

653

654 **Data availability**

655 Meteorological (station: delsjmet-p) and water quality (station: Aspen Landing) data are

656 available from the National Estuarine Research Reserve's Centralized Data Management Office

657 (CDMO) at https://cdmo.baruch.sc.edu/. Phenological data are available from the PhenoCam

658 network (site: stjones) at https://phenocam.sr.unh.edu/webcam/sites/stjones/. Data from trace gas

659 fluxes ~~will be publicly~~are available in ~~a FAIR data repository (e.g.,~~ Figshare~~) before publication~~

660 ~~of this research.~~ (doi:10.6084/m9.figshare.20449131).

661

662 **Author contributions**

663 MC and RV conceptualized the study, designed the methodology, and conducted project

664 administration. MC conducted the formal analysis, investigation, and visualization, as well as

665 wrote the original draft. RV provide funding, resources, supervision, as well as reviewed and

666 edited the manuscript.

667

668 **Competing interests**

669   ——————The authors declare that they have no conflict of interest.

670

671

References

Al-Haj, A. N. and Fulweiler, R. W.: A synthesis of methane emissions from shallow vegetated coastal ecosystems, Glob. Chang. Biol., 26, 2988–3005, https://doi.org/10.1111/gcb.15046, 2020.

Andreae, M. O. and Jaeschke, W. A.: Exchange of sulfur between biosphere and atmosphere over temperate and tropical regions, in: Sulfur Cycling on the Continents, edited by: Howarth, R. W., Stewart, J. W. B., and Ivanov, M. V., Wiley, New York, 1992.

Bahlmann, E., Weinberg, I., Lavrič, J. V, Eckhardt, T., Michaelis, W., Santos, R., and Seifert, R.: Tidal controls on trace gas dynamics in a seagrass meadow of the Ria Formosa lagoon (southern Portugal), 12, 1683–1696, https://doi.org/10.5194/bg-12-1683-2015, 2015.

Barba, J., Cueva, A., Bahn, M., Barron-Gafford, G. A., Bond-Lamberty, B., Hanson, P. J., Jaimes, A., Kulmala, L., Pumpanen, J., Scott, R. L., Wohlfahrt, G., and Vargas, R.: Comparing ecosystem and soil respiration: reviewReview and key challenges of tower-based and soil measurements, Agric. For. Meteorol., 249, 434–443, https://doi.org/10.1016/j.agrformet.2017.10.028, 2018.

Barbier, E., Hacker, S., Kennedy, C., Stier, A., and Silliman, B.: The value of estuarine and coastal ecosystem services, Ecol. Monogr., 81, 169–193, 2011.

Bartlett, K. B., Harriss, R. C., and Sebacher, D. I.: Methane fluxFlux from coastal salt marshesCoastal Salt Marshes, J. Geophys. Res., 90, 5710–5720, 1985.

Bauza, J. F., Morell, J. M., and Corredor, J. E.: Biogeochemistry of nitrous oxide production in the red mangrove (Rhizophora mangle) forest sediments, Estuar. Coast. Shelf Sci., 55, 697–704, https://doi.org/10.1006/ecss.2001.0913, 2002.

Bridgham, S. D. and Richardson, C. J.: Mechanisms controlling soil respiration (CO2 and CH4) in southern peatlands, Soil Biol. Biochem., 24, 1089–1099, https://doi.org/10.1016/0038-0717(92)90058-6, 1992.

Brimblecombe, P.: The Global Sulfur Cycle, in: Treatise on Geochemistry, vol. 10, edited by:

Holland, H. D. and Turekian, K. K., Elsevier Science, 559–591,

https://doi.org/10.1016/B978-0-08-095975-7.00814-7, 2014.

Brühl, C., Lelieveld, J., Crutzen, P. J., and Tost, H.: The role of carbonyl sulphide as a source of stratospheric sulphate aerosol and its impact on climate, Atmos. Chem. Phys., 12, 1239–1253, https://doi.org/10.5194/acp-12-1239-2012, 2012.

Capone, D. G. and Kiene, R. P.: Comparison of microbial dynamics in marine and freshwater sediment, Limnol. Ocean., 33, 725–749, 1988.

714   Capooci, M. and Vargas, R.: Diel and seasonal patterns of soil CO2 efflux in a temperate tidal
715   marsh, Sci. Total Environ., 802, https://doi.org/10.1016/j.scitotenv.2021.149715, 2022.

716   Capooci, M., Barba, J., Seyfferth, A. L., and Vargas, R.: Experimental influence of storm-surge
717   salinity on soil greenhouse gas emissions from a tidal salt marsh, Sci. Total Environ.,
718   686, 1164–1172, https://doi.org/10.1016/j.scitotenv.2019.06.032, 2019.

719   Carroll, M. A., Heidt, L. E., Cicerone, R. J., and Prinn, R. G.: OCS, H2S, and CS2 fluxes from
720   a salt water marsh, J. Atmos. Chem., 4, 375–395, https://doi.org/10.1007/BF00053811,
721   1986.

722   Charlson, R. J., Lovelock, J. E., Andreae, M. O., and Warren, S. G.: Oceanic phytoplankton,
723   atmospheric sulphur, cloud albedo and climate, Nature, 326, 655–661,
724   https://doi.org/10.1038/326655a0, 1987.

725   Cheng, X., Peng, R., Chen, J., Luo, Y., Zhang, Q., An, S., Chen, J., and Li, B.: CH4 and N2O
726   emissions from Spartina alterniflora and Phragmites australis in experimental
727   mesocosms, Chemosphere, 68, 420–427,
728   https://doi.org/10.1016/J.CHEMOSPHERE.2007.01.004, 2007.

729   Cooper, D. J., De Mello, W. Z., Cooper, W. J., Zika, R. G., Saltzman, E. S., Prospero, J. M.,
730   and Savoie, D. L.: Short-term variability in biogenic sulphur emissions from a Florida
731   Spartina alterniflora marsh, Atmos. Environ., 21, 7–12, 1987a.

732   Cooper, W. J., Cooper, D. J., Saltzman, E. S., Mello, W. Z. d., Savoie, D. L., Zika, R. G., and
733   Prospero, J. M.: Emissions of biogenic sulphur compounds from several wetland soils
734   in Florida, Atmos. Environ., 21, 1491–1495, https://doi.org/10.1016/0004-
735   6981(87)90311-8, 1987b.

736   Dacey, J. W. H., King, G. M., and Wakeham, S. G.: Factors controlling emission of
737   dimethylsulphide from salt marshes, Nature, 330, 643–645,
738   https://doi.org/10.1038/330643a0, 1987.

739   DeLaune, R. D., Devai, I., and Lindau, C. W.: Flux of reduced sulfur gases along a salinity
740   gradient in Louisiana coastal marshes, Estuar. Coast. Shelf Sci., 54, 1003–1011,
741   https://doi.org/10.1006/ecss.2001.0871, 2002.

742   Diefenderfer, H. L., Cullinan, V. I., Borde, A. B., Gunn, C. M., and Thom, R. M.: High-
743   frequency greenhouse gas flux measurement system detects winter storm surge effects
744   on salt marsh, Glob. Chang. Biol., 24, 5961–5971, https://doi.org/10.1111/gcb.14430,
745   2018.

746   DNREC: Delaware National Esturaine Research Reserve Estuarine Profile, 158 pp., 1999.

747   Duarte, C. M., Middelburg, J. J., and Caraco, N.: Major role of marine vegetation on the
748   oceanic carbon cycle, 2, 1–8, https://doi.org/10.1111/j.2042-7158.1975.tb10261.x,
749   2005.

750 Emery, H. E. and Fulweiler, R. W.: Spartina alterniflora and invasive Phragmites australis
751   stands have similar greenhouse gas emissions in a New England marsh, Aquat. Bot.,
752   116, 83–92, https://doi.org/10.1016/j.aquabot.2014.01.010, 2014.

753 Emmer, I., Needelman, B., Emmett-Mattox, S., Crooks, S., Beers, L., Megonigal, P., Myers,
754   D., Oreska, M., McGlathery, K., and Shoch, D.: Methodology for tidal wetlandTidal
755   Wetland and seagrass restorationSeagrass Restoration, 1–115 pp., 2021.

756 Filippa, G., Cremonese, E., Migliavacca, M., Galvagno, M., Folker, M., Richardson, A. D., and
757   Tomelleri, E.: phenopix: process digital imagesProcess Digital Images of a vegetation
758   coverVegetation Cover, R PackagePackag. version 2.4.2, 2020.

759 Finster, K., King, G. M., Bak, F., and Finster, K.: Formation of methylmercaptan and
760   dimethylsulfide from methoxylated aromatic compounds in anoxic marine and fresh
761   water sediments, FEMS Microbiol. Ecol., 74, 295–302, https://doi.org/10.1111/j.1574-
762   6968.1990.tb04076.x, 1990.

763 Goldan, P. D., Kuster, W. C., Albritton, D. L., and Fehsenfeld, F. C.: The measurement of
764   natural sulfur emissions from soils and vegetation: threeThree sites in the Eastern
765   United States revisited, J. Atmos. Chem., 5, 439–467,
766   https://doi.org/10.1007/BF00113905, 1987.

767 Granville, K. E., Ooi, S. K., Koenig, L. E., Lawrence, B. A., Elphick, C. S., and Helton, A. M.:
768   Seasonal patternsPatterns of denitrificationDenitrification and N2O
769   productionProduction in a southernSouthern New England salt marshSalt Marsh, 41, 1–
770   13, https://doi.org/10.1007/s13157-021-01393-x, 2021.

771 Hill, A. C. and Vargas, R.: Methane and Carbon Dioxide Fluxes in a Temperate Tidal Salt
772   Marsh: Comparisons Between Plot and Ecosystem Measurements, J. Geophys. Res.
773   Biogeosciences, 127, e2022JG006943, https://doi.org/10.1029/2022JG006943, 2022.

774 Hill, A. C., Vázquez-Lule, A., and Vargas, R.: Linking vegetation spectral reflectance with
775   ecosystem carbon phenology in a temperate salt marsh, Agric. For. Meteorol., 307,
776   108481, https://doi.org/10.1016/j.agrformet.2021.108481, 2021.

777 Hines, M. E.: Emissions of sulfur gases from wetlands, 25, 153–161,
778   https://doi.org/10.1080/05384680.1996.11904076, 1996.

779 Järveoja, J., Nilsson, M. B., Gažovič, M., Crill, P. M., and Peichl, M.: Partitioning of the net
780   CO2 exchange using an automated chamber system reveals plant phenology as key
781   control of production and respiration fluxes in a boreal peatland, Glob. Chang. Biol., 24,
782   3436–3451, https://doi.org/10.1111/gcb.14292, 2018.

783 Jha, C. S., Rodda, S. R., Thumaty, K. C., Raha, A. K., and Dadhwal, V. K.: Eddy covariance
784   based methane flux in Sundarbans mangroves, India, J. Earth Syst. Sci., 123, 1089–
785   1096, https://doi.org/10.1007/s12040-014-0451-y, 2014.

786 Jørgensen, B. B. and Okholm-Hansen, B.: Emissions of biogenic sulfur gases from a

787   ~~Danish~~danish estuary, Atmos. Environ., 19, 1737–1749, https://doi.org/10.1016/0004-
788   6981(85)90001-0, 1985.

789   Kellogg, W. W., Cadle, R. D., Allen, E. R., Lazrus, A. L., and Martell, E. A.: The Sulfur Cycle,
790   Science~~., 4022 ((80-.)., 175),,~~ 587–596, https://doi.org/10.1016/S0074-6142(08)62696-
791   0, 1972.

792   Kiene, R. P.: Dimethyl sulfide metabolism in salt marsh sediments, FEMS Microbiol. Lett., 53,
793   71–78, https://doi.org/10.1016/0378-1097(88)90014-6, 1988.

794   Kiene, R. P. and Visscher, P. T.: Production and fate of methylated sulfur
795   ~~compounds~~mompounds from methionine and dimethylsulfoniopropionate in anoxic salt
796   marsh ~~Sediments~~sediments, Appl. Environ. Microbiol., 53, 2426–2434, 1987.

797   Kim, J., Verma, S. B., Billesbach, D. P., and Clement, R. J.: Diel variation in methane emission
798   from a midlatitude prairie wetland: ~~significance~~Significance of convective throughflow
799   in Phragmites australis, J. Geophys. Res. Atmos., 103, 28029–28039,
800   https://doi.org/10.1029/98JD02441, 1998.

801   Koskinen, M., Minkkinen, K., Ojanen, P., Kämäräinen, M., Laurila, T., and Lohila, A.:
802   Measurements of CO2 exchange with an automated chamber system throughout the
803   year: Challenges in measuring night-time respiration on porous peat soil, 11, 347–363,
804   https://doi.org/10.5194/bg-11-347-2014, 2014.

805   Laursen, A. E. and Seitzinger, S. P.: Measurement of denitrification in rivers: an integrated,
806   whole reach approach, Hydrobiologia, 485, 67–81, 2002.

807   Lin, Y. S., Heuer, V. B., Ferdelman, T. G., and Hinrichs, K.-U.: Microbial conversion of
808   inorganic carbon to dimethyl sulfide in anoxic lake sediment (Plußsee, Germany), 7,
809   2433–2444, https://doi.org/10.5194/bg-7-2433-2010, 2010.

810   Livesley, S. J. and Andrusiak, S. M.: Temperate mangrove and salt marsh sediments are a small
811   methane and nitrous oxide source but important carbon store, Estuar. Coast. Shelf Sci.,
812   97, 19–27, https://doi.org/10.1016/j.ecss.2011.11.002, 2012.

813   Lomans, B. P., Van der Drift, C., Pol, A., and Op den Camp, H. J. M.: Microbial cycling of
814   volatile organic sulfur compounds, Water Sci. Technol., 45, 55–60,
815   https://doi.org/10.1007/s00018-002-8450-6, 2002.

816   Macreadie, P. I., Costa, M. D. P., Atwood, T. B., Friess, D. A., Kelleway, J. J., Kennedy, H.,
817   Lovelock, C. E., Serrano, O., and Duarte, C. M.: Blue carbon as a natural climate
818   solution, Nat. Rev. Earth Environ., 2, 826–839,
819   https://doi.org/https://doi.org/10.1038/s43017-021-00224-1, 2021.

820   McTigue, N. D., Walker, Q. A., and Currin, C. A.: Refining Estimates of Greenhouse Gas
821   Emissions From Salt Marsh "Blue Carbon" Erosion and Decomposition, Front. Mar.
822   Sci., 8, 1–13, https://doi.org/10.3389/fmars.2021.661442, 2021.

De Mello, W. Z., Cooper, D. J., Cooper, W. J., Saltzman, E. S., Zika, R. G., Savoie, D. L., and Prospero, J. M.: Spatial and diel variability in the emissions of some biogenic sulfur compounds from a Florida Spartina alterniflora coastal zone, Atmos. Environ., 21, 987–990, https://doi.org/10.1016/0004-6981(87)90095-3, 1987.

Middelburg, J. J., Klaver, G., Nieuwenhuize, J., Wielemaker, A., de Hass, W. De, Vlug, T., Nat, J. F. W. A. Van Der, Middelburg, J. J., Klaver, G., Haas, W. De,., Vlug, T., and Jaco, Fvan der Nat, J. F. W. A.: Organic matter mineral sediments along an estuarine gradient, Mar. Ecol. Prog. Ser., 132, 157–168, 1996.

Moffett, K. B., Wolf, A., Berry, J. A., and Gorelick, S. M.: Salt marsh-atmosphere exchange of energy, water vapor, and carbon dioxide: Effects of tidal flooding and biophysical controls, 46, https://doi.org/10.1029/2009WR009041, 2010.

Möller, I., Kudella, M., Rupprecht, F., Spencer, T., Paul, M., Van Wesenbeeck, B. K., Wolters, G., Jensen, K., Bouma, T. J., Miranda-Lange, M., and Schimmels, S.: Wave attenuation over coastal salt marshes under storm surge conditions, Nat. Geosci., 7, 727–731, https://doi.org/10.1038/NGEO2251, 2014.

Moran, J. J., House, C. H., Vrentas, J. M., and Freeman, K. H.: Methyl sulfide production by a novel carbon monoxide metabolism in Methanosarcina acetivorans, Appl. Environ. Microbiol., 74, 540–542, https://doi.org/10.1128/AEM.01750-07, 2008.

Morrison, M. C. and Hines, M. E.: The variability of biogenic sulfur flux from a temperate salt marsh on short time and space scales, Atmos. Environ. Part A. Gen. Top., 24A, 1771–1779, https://doi.org/10.1016/0960-1686(90)90509-L, 1990.

Moseman-Valtierra, S., Gonzalez, R., Kroeger, K. D., Tang, J., Chao, W. C., Crusius, J., Bratton, J., Green, A., and Shelton, J.: Short-term nitrogen additions can shift a coastal wetland from a sink to a source of N2O, Atmos. Environ., 45, 4390–4397, https://doi.org/10.1016/j.atmosenv.2011.05.046, 2011.

Moseman-Valtierra, S., Abdul-Aziz, O. I., Tang, J., Ishtiaq, K. S., Morkeski, K., Mora, J., Quinn, R. K., Martin, R. M., Egan, K., Brannon, E. Q., Carey, J., and Kroeger, K. D.: Carbon dioxide fluxes reflect plant zonation and belowground biomass in a coastal marsh, 7, e01560, 2016.

Murray, R. H., Erler, D. V., and Eyre, B. D.: Nitrous oxide fluxes in estuarine environmentsenvironments : response to global change, Glob. Chang. Biol., 21, 3219–3245, https://doi.org/10.1111/gcb.12923, 2015.

Van Der Nat, F. and Middelburg, J. J.: Methane emission from tidal freshwater marshes, Biogeochemistry, 49, 103–121, 2000.

Neubauer, S. C. and Megonigal, J. P.: Correction to: Moving Beyond Global Warming Potentials to Quantify the Climatic Role of Ecosystems, Ecosyst. 2019 228, 22, 1931–1932, https://doi.org/10.1007/S10021-019-00422-5, 2019.

NOAA National Estuarine Research Reserve System (NERRS).: System-wide monitoring program, 2015System-wide Monitoring Program:

Oremland, R. S., Marsh, L. M., and Polcin, S.: Methane production and simultaneous sulphate reduction in anoxic, salt marsh sediments, Nature, 296, 143–145, 1982.

Peterson, P. M., Romaschenko, K., Arrieta, Y. H., and Saarela, J. M.: A molecular phylogeny and new subgeneric classification of Sporobolus (Poaceae: Chloridoideae: Sporobolinae), Taxon, 63, 1212–1243, https://doi.org/10.12705/636.19, 2014.

Petrakis, S., Seyfferth, A., Kan, J., Inamdar, S., and Vargas, R.: Influence of experimental extreme water pulses on greenhouse gas emissions from soils, Biogeochemistry, 133, 147–164, https://doi.org/10.1007/s10533-017-0320-2, 2017.

Rinne, J., Riutta, T., Pihlatie, M., Aurela, M., Haapanala, S., Tuovinen, J. P., Tuittila, E. S., and Vesala, T.: Annual cycle of methane emission from a boreal fen measured by the eddy covariance technique, Tellus, Ser. B Chem. Phys. Meteorol., 59, 449–457, https://doi.org/10.1111/j.1600-0889.2007.00261.x, 2007.

Rosentreter, J. A., Maher, D. T., Erler, D. V., Murray, R. H., and Eyre, B. D.: Methane emissions partially offset "blue carbon" burial in mangroves, Sci. Adv., 4, eaao4985, https://doi.org/10.1126/SCIADV.AAO4985, 2018.

Rosentreter, J. A., Al-Haj, A. N., Fulweiler, R. W., and Williamson, P.: Methane and nitrous oxide emissions complicate coastal blue carbon assessmentsNitrous Oxide Emissions Complicate Coastal Blue Carbon Assessments, Global Biogeochem. Cycles, 35, e2020GB006858, https://doi.org/10.1029/2020GB006858, 2021.

Savage, K., Phillips, R., and Davidson, E.: High temporal frequency measurements of greenhouse gas emissions from soils, 11, 2709–2720, https://doi.org/10.5194/bg-11-2709-2014, 2014.

Sela-Adler, M., Said-Ahmad, W., Sivan, O., Eckert, W., Kiene, R. P., and Amrani, A.: Isotopic evidence for the origin of dimethylsulfide and dimethylsulfoniopropionate-like compounds in a warm, monomictic freshwater lake, Environ. Chem., 13, 340–351, https://doi.org/https://doi.org/10.1071/EN15042, 2015.

Seyednasrollah, B., Young, A. M., Hufkens, K., Milliman, T., Friedl, M. A., Frolking, S., Richardson, A. D., Abraha, M., Allen, D. W., Apple, M., Arain, M. A., Baker, J., Baker, J. M., Baldocchi, D., Bernacchi, C. J., Bhattacharjee, J., Blanken, P., Bosch, D. D., Boughton, R., Boughton, E. H., [...]and Zona, D.: PhenoCam dataset v2.0: Vegetation phenology from digital camera imagery, Oak Ridge, Tennessee, https://doi.org/https://doi.org/10.3334/ ORNLDAAC/1674, 2019.

Seyfferth, A. L., Bothfeld, F., Vargas, R., Stuckey, J. W., Wang, J., Kearns, K., Michael, H. A., Guimond, J., Yu, X., and Sparks, D. L.: Spatial and temporal heterogeneity of geochemical controls on carbon cycling in a tidal salt marsh, Geochim. Cosmochim. Acta, 282, 1–18, https://doi.org/10.1016/j.gca.2020.05.013, 2020.

898   Simpson, L. T., Osborne, T. Z., and Feller, I. C.: Wetland ~~soil~~Soil CO2 ~~efflux along~~Efflux
899   Along a ~~latitudinal gradient~~Latitudinal Gradient of ~~spatial~~Spatial and ~~temporal~~
900   ~~complexity~~Temporal Complexity, 42, 45–54, https://doi.org/10.1007/s12237-018-0442-
901   3, 2019.

902   Steudler, P. A. and Peterson, B. J.: Contribution of gaseous sulphur from salt marshes to the
903   global sulphur cycle, Nature, 311, 455–457, https://doi.org/10.1038/311455a0, 1984.

904   Steudler, P. A. and Peterson, B. J.: Annual cycle of gaseous sulfur emissions from a New
905   England Spartina alterniflora marsh, Atmos. Environ., 19, 1411–1416,
906   https://doi.org/10.1016/0004-6981(85)90278-1, 1985.

907   Taubman, S. J. and Kasting, J. F.: Carbonyl sulfide: ~~no~~No remedy for global warming,
908   Geophys. Res. Lett., 22, 803–805, https://doi.org/10.1029/95GL00636, 1995.

909   Thomas, M. A., Suntharalingam, P., Pozzoli, L., Rast, S., Devasthale, A., Kloster, S., Feichter,
910   J., and Lenton, T. M.: Quantification of DMS aerosol-cloud-climate interactions using
911   the ECHAM5-HAMMOZ model in a current climate scenario, Atmos. Chem. Phys., 10,
912   7425–7438, https://doi.org/10.5194/acp-10-7425-2010, 2010.

913   Tong, C., Huang, J. F., Hu, Z. Q., and Jin, Y. F.: Diurnal ~~variations of carbon dioxide, methane,~~
914   ~~and nitrous oxide vertical fluxes in a subtropical estuarine marsh on neap~~Variations of
915   Carbon Dioxide, Methane, and ~~spring tide days~~Nitrous Oxide Vertical Fluxes in a
916   Subtropical Estuarine Marsh on Neap and Spring Tide Days, 36, 633–642,
917   https://doi.org/10.1007/s12237-013-9596-1, 2013.

918   Tong, C., Morris, J. T., Huang, J., Xu, H., and Wan, S.: Changes in pore-water chemistry and
919   methane emission following the invasion of Spartina alterniflora into an oliogohaline
920   marsh, Limnol. Oceanogr., 63, 384–396, https://doi.org/10.1002/lno.10637, 2018.

921   Trifunovic, B., Vázquez-Lule, A., Capooci, M., Seyfferth, A. L., Moffat, C., and Vargas, R.:
922   Carbon ~~dioxide~~Dioxide and ~~methane emissions from temperate salt marsh tidal~~
923   ~~creek~~Methane Emissions From Temperate Salt Marsh Tidal Creek, J. Geophys. Res.
924   Biogeosciences, 125, https://doi.org/10.1029/2019JG005558, 2020.

925   Turetsky, M. R., Kotowska, A., Bubier, J., Dise, N. B., Crill, P., Hornibrook, E. R. C.,
926   Minkkinen, K., Moore, T. R., Myers-Smith, I. H., Nykanen, H., Olefeldt, D., Rinne, J.,
927   Saarnio, S., Shurpali, N., Tuittila, E. S., Waddington, J. M., White, J. R., Wickland, K.
928   P., and Wilmking, M.: A synthesis of methane emissions from 71 northern, temperate,
929   and subtropical wetlands, Glob. Chang. Biol., 20, 2183–2197,
930   https://doi.org/10.1111/gcb.12580, 2014.

931   UNFCCC: Paris Agreement, 2015.

932   Vargas, R., Carbone, M. S., Reichstein, M., and Baldocchi, D. D.: Frontiers and challenges in
933   soil respiration research: from measurements to model-data integration,
934   Biogeochemistry, 102, 1–13, https://doi.org/10.1007/s10533-010-9462-1, 2011.

Vázquez-Lule, A. and Vargas, R.: Biophysical drivers of net ecosystem and methane exchange
across phenological phases in a tidal salt marsh, Agric. For. Meteorol., 300,
https://doi.org/10.1016/j.agrformet.2020.108309, 2021.

Wang, J. and Wang, J.: Spartina alterniflora alters ecosystem DMS and CH4 emissions and
their relationship along interacting tidal and vegetation gradients within a coastal salt
marsh in Eastern China, Atmos. Environ., 167, 346–359,
https://doi.org/10.1016/J.ATMOSENV.2017.08.041, 2017.

Ward, N., Megonigal, P. J., Bond-Lamberty, B., Bailey, V., Butman, D., Canuel, E.,
Diefenderfer, H., Ganju, N. K., Goñi, M. A., Graham, E. B., Hopkinson, C. S.,
Khangaonkar, T., Langley, J. A., McDowell, N. G., Myers-Pigg, A. N., Neumann, R.
B., Osburn, C. L., Price, R. M., Rowland, J., Sengupta, A., Simard, M., Thornton, P. E.,
Tzortziou, M., Vargas, R., Weisenhorn, P. B., and Windham-Myers, L.: Representing
the ~~function~~Function and ~~sensitivity~~Sensitivity of ~~coastal interfaces~~Coastal Interfaces in
~~earth system models~~Earth System Models, Nat. Commun., 11~~, 1–14~~,
https://doi.org/10.1038/s41467-020-16236-2, 2020.

Watts, S. F.: The mass budgets of carbonyl sulfide, dimethyl sulfide, carbon disulfide and
hydrogen sulfide, Atmos. Environ., 34, 761–779, https://doi.org/10.1016/S1352-
2310(99)00342-8, 2000.

Whelan, M. E., Min, D. H., and Rhew, R. C.: Salt marsh vegetation as a carbonyl sulfide (COS)
source to the atmosphere, Atmos. Environ., 73, 131–137,
https://doi.org/10.1016/J.ATMOSENV.2013.02.048, 2013.

Wilson, B. J., Mortazavi, B., and Kiene, R. P.: Spatial and temporal variability in carbon
dioxide and methane exchange at three coastal marshes along a salinity gradient in a
northern Gulf of Mexico estuary, Biogeochemistry, 123, 329–347,
https://doi.org/10.1007/s10533-015-0085-4, 2015.

Xie, H. and Moore, R. M.: Carbon disulfide in the North Atlantic and Pacific Oceans, J.
Geophys. Res. Ocean., 104, 5393–5402, https://doi.org/10.1029/1998jc900074, 1999.

Xie, X., Zhang, M.-Q., Zhao, B., and Guo, H.-Q.: Dependence of coastal wetland ecosystem
respiration on temperature and tides: a temporal perspective, 11, 539–545,
https://doi.org/10.5194/bg-11-539-2014, 2014.

Xu, X., Fu, G., Zou, X., Ge, C., and Zhao, Y.: Diurnal variations of carbon dioxide, methane,
and nitrous oxide fluxes from invasive Spartina alterniflora dominated coastal wetland
in northern Jiangsu Province, Acta Oceanol. Sin., 36, 105–113,
https://doi.org/10.1007/s13131-017-1015-1, 2017.

Yang, W.-B., Yuan, C.-S., Huang, B.-Q., Tong, C., and Yang, L.: Emission
~~characteristics~~Characteristics of ~~greenhouse gases~~Greenhouse Gases and ~~their~~
~~correlation~~Their Correlation with ~~water quality~~Water Quality at an ~~estuarine mangrove~~
~~ecosystem~~Estuarine Mangrove Ecosystem – the ~~application~~Application of an ~~in~~In-situ
~~on~~On-site NDIR ~~monitoring technique~~Monitoring Technique, Wetl. 2018 384, 38, 723–

738, https://doi.org/10.1007/S13157-018-1015-8, 2018.

Yang, W.-B. Bin, Yuan, C.-S. S., Tong, C., Yang, P., Yang, L., and Huang, B.-Q. Q.: Diurnal variation of CO2, CH4, and N2O emission fluxes continuously monitored in-situ in three environmental habitats in a subtropical estuarine wetland, Mar. Pollut. Bull., 119, 289–298, https://doi.org/10.1016/j.marpolbul.2017.04.005, 2017.

Yu, X., Ye, S., Olsson, L., Wei, M., Krauss, K. W., and Brix, H.: A 3-~~year in-situ measurement~~Year In-Situ Measurement of ~~CO₂ efflux in coastal wetlands: understanding carbon loss~~CO 2 Efflux in Coastal Wetlands: Understanding Carbon Loss through ~~ecosystem respiration~~Ecosystem Respiration and its ~~partitioning~~Partitioning, https://doi.org/10.1007/s13157-019-01197-0, 2019.

Yu, Z., Li, Y., Deng, H., Wang, D., Chen, Z., and Xu, S.: Effect of Scirpus mariqueter on nitrous oxide emissions from a subtropical monsoon estuarine wetland, J. Geophys. Res. Biogeosciences, 117, 2017, https://doi.org/10.1029/2011JG001850, 2012.

Zhang, Y. and Ding, W.: Diel methane emissions in stands of Spartina alterniflora and Suaeda salsa from a coastal salt marsh, Aquat. Bot., 95, 262–267, https://doi.org/10.1016/j.aquabot.2011.08.005, 2011.

Zhang, Y., Wang, L., Xie, X., Huang, L., and Wu, Y.: Effects of invasion of Spartina alterniflora and exogenous N deposition on N2O emissions in a coastal salt marsh, Ecol. Eng., 58, 77–83, https://doi.org/10.1016/j.ecoleng.2013.06.011, 2013.